Technical Physics Letters, 2023, Vol. 49, No. 7

07.1

Resistivity of thin-film electrodes Si@O@Al and $LiCoO_2$

© A.S. Rudy, S.V. Kurbatov, A.A. Mironenko, V.V. Naumov, Yu.S. Egorova, E.A. Kozlov

Demidov State University, Yaroslavl, Russia
E-mail: rudy@uniyar.ac.ru

Received February 28, 2023
Revised April 19, 2023
Accepted May 10, 2023

The results of measuring the resistivity of thin-film structures Ti—Si@O@Al—Ti and Ti—$LiCoO_2$—Ti by electrochemical impedance spectroscopy (EIS) and cyclic voltammetry (CV) are presented. It was found that, according to the EIS data, the resistance of Ti—Si@O@Al—Ti is three orders of magnitude higher than the CV data, which is due to the nonohmic nature of the metal-semiconductor junction and the varistor effect. It is shown that the Ti−$LiCoO_2$ contact is ohmic, while the nonlinearity of the CVC is well described by the varistor effect. The results obtained are of importance for the interpretation of the impedance spectra of thin-film solid-state lithium-ion batteries based on semiconductor materials.

Keywords: Thin-film electrode, impedance spectroscopy, cyclic voltammetry, metal−semiconductor junction, varistor effect.

DOI: 10.61011/TPL.2023.07.56444.19543

Lithium cobaltite $LiCoO_2$ currently remains the most commonly used material for positive electrodes of thin-film solid-state lithium-ion batteries (TSLIBs). It is well known as the first and the most commercially viable material for lithium-ion batteries. Among the possible the materials for negative electrodes, silicon has the greatest capacity [1–6], while nanocomposite Si@O@Al provides the best performance figures. It is less known, since it has been developed in Russia [7] and is not used in commercial TSLIBs. However, offering a high specific capacity of $3000-3500\,\mathrm{A\cdot h/g}$ and withstanding more than 1000 charge-discharge cycles, Si@O@Al has potential for wide application. The key parameter of such materials is their resistivity, which does also depend on the degree of lithiation. Therefore, the results of measurement of the electrode resistance in TSLIBs are of special interest. The method of electrochemical impedance spectroscopy (EIS), which may yield greatly overestimated values for nonlinear semiconductor electrodes, is typically used to perform these measurements. For example, a structural model of a TSLIB of the $LiCoO_2$−LiPON−Si@O@Al electrochemical system proposed in [8] characterized the EIS results well. At the same time, the resistances of electrodes obtained by fitting were much higher than the ones determined using cyclic voltammetry (CV) for the Ti—Si@O@Al—Ti structure [9] and the EIS resistances for bulk $LiCoO_2$ samples [10]. This discrepancy may be attributed to the fact that metal−semiconductor junctions were not identified as separate structural elements in the model from [8] (and in similar studies carried out by other research groups [11–14]). In order to verify this assumption, we measured the impedance and current-voltage curves (CVCs) of test Ti—Si@O@Al—Ti and Ti—$LiCoO_2$—Ti structures.

Test structures were fabricated by magnetron sputtering using an SCR 651 Tetra (Alcatel) setup. Layers of Ti, Si@O@Al, and $LiCoO_2$ were deposited onto a Si—SiO_2 substrate through a mask (the window size was 10×10 mm). The technological parameters of synthesis of test structures are listed in the table. Impedance measurements were performed using the four-point probe technique and an Elins P-40X single-channel potentiostat with an FRA-24M electrochemical impedance measurement module. The voltage amplitude was 5 mV, and the frequency range spanned from 500 kHz to 500 mHz. Spectra were recorded in a single pass from higher frequencies to lower ones.

Figure 1 presents the Nyquist plots for the Ti—Si@O@Al—Ti test structure obtained at a temperature of $+24^\circ$C under various bias voltages relative to a normally open circuit. It can be seen that the resistance of the Ti—Si@O@Al—Ti structure under zero bias is $R=7.52\,\mathrm{k\Omega}$, whereas the resistance of the same structure under a bias of 1 V reported in [9] was just $6.26\,\Omega$. The values from [9] are the result of approximation of CVCs and are thus more reliable. The indicated discrepancy is attributable to the varistor effect and the additional resistance of a metal−semiconductor contact. It was demonstrated in [9] that the CVC of the Ti−Si@O@Al junction under backward bias is exponential in nature. At voltage amplitude $U_A=5$ mV, the amplitude of current through the contact is on the order of the saturation current. The maximum values of the real impedance part (maxReZ) in EIS spectra are overestimated greatly as a result.

Technological parameters of synthesis of lithium cobaltite samples

Layer	Target	Flow rate of Ar, sccm	Flow rate of O_2, sccm	Purification	Pressure, Pa	Magnetron power, W	Time, min	Thickness, nm
Ti		20	–	–	0.2	300	10	200
$LiCoO_2$	$LiCoO_2$ (99.9%)	20	5	15 V, 15 s	10	200	100	500
Si@O@Al	Si_3Al	200	0.6	15 V, 15 s	1.75	400	4	180

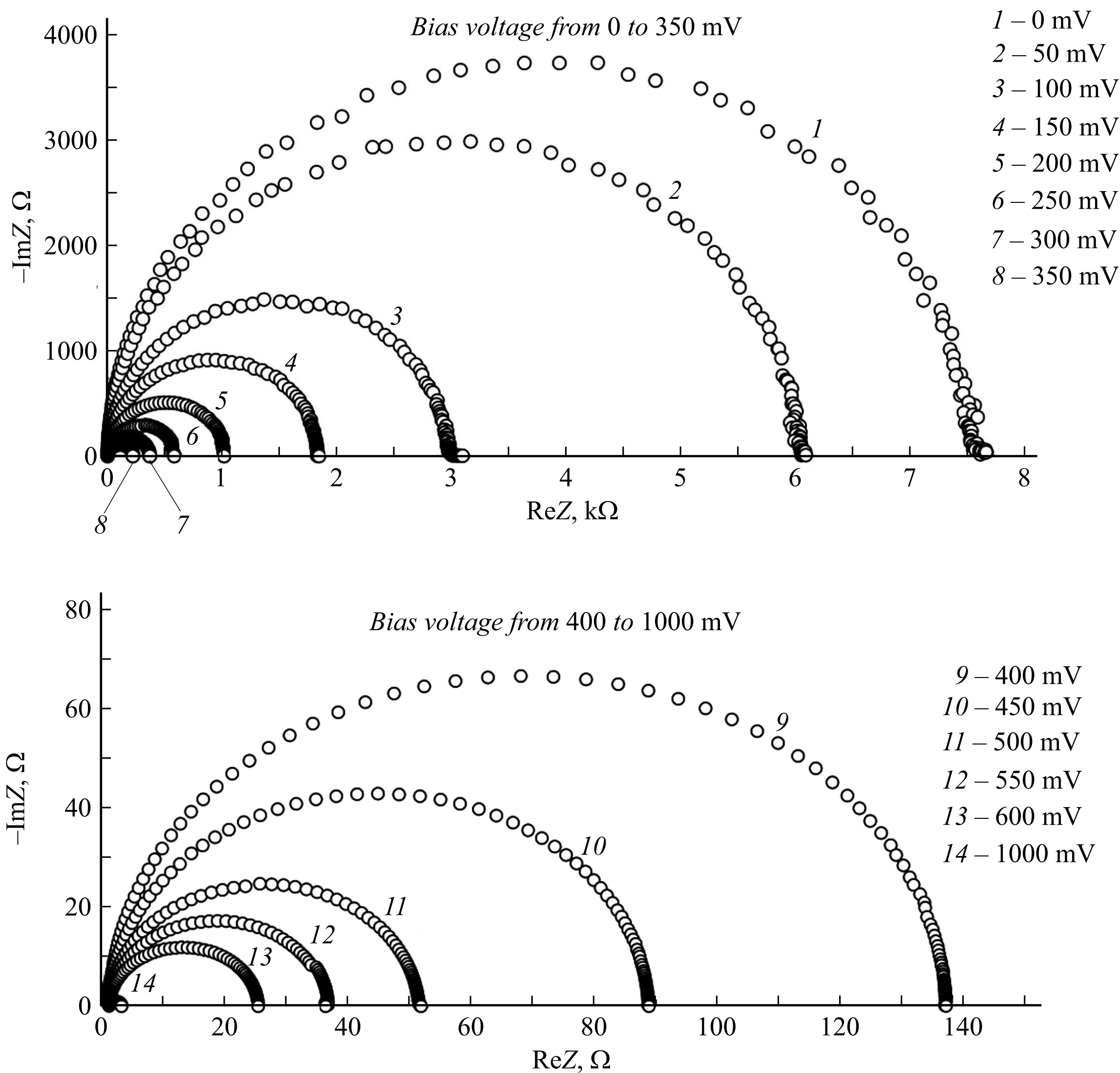

Figure 1. Nyquist plots for the Ti—Si@O@Al—Ti test structure under various bias voltages.

In view of the above, the diameters of circles in Fig. 1 should decrease (due to a reduction in the contact resistance and weakening of the varistor effect) with increasing bias voltage. The sign of this bias voltage is insignificant, since one junction will be biased in the forward direction and its characteristic will remain linear. The second junction will be biased in the backward direction (i.e., into the region with a steeper CVC slope). The differential contact resistance will decrease as a result, and the circle in a Nyquist plot will contract. The validity of these assumptions is verified by the impedance spectra in Fig. 1 obtained under bias voltages ranging from 0 to 1 V. The

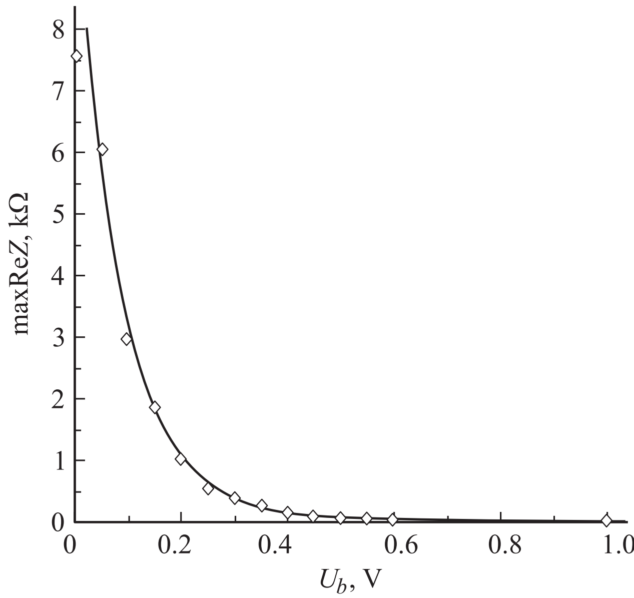

Figure 2. Experimental dependence $\mathrm{Re}Z(U_b)$ (dots) and approximating dependence (solid curve) at parameters $I_S = 2.75 \cdot 10^{-6}$ A, $b = 0.68$, and $R_0 = 3.00\,\Omega$. Parameters $\mathcal{R} = 1.56\,\Omega \cdot \mathrm{A}^{1-\alpha}$ and $\alpha = 0.45$ were taken from [3].

dependence of maxReZ on the bias voltage is presented in Fig. 2.

An analytical expression for the $\mathrm{maxRe}Z(U_b)$ dependence may be derived from relation

$$I = I_S\left(e^{(U_b - U_V)/\phi} - 1\right), \tag{1}$$

a more convenient form of which is

$$U_b - U_V = f \ln(1 + I/I_S),$$

where $f = k_B T/q$, I_S is the saturation current, U_b is the bias voltage, and U_V is the voltage drop in the bulk. Taking the Si@O@Al varistor effect into account, one may write $U_V = \mathcal{R} I^\alpha + R_0 I$, where $\mathcal{R}$ is a coefficient with a dimension of $\Omega \cdot \mathrm{A}^{1-\alpha}$. The current dependence of the bias then takes the form $U_b = \phi \ln(1 + I/I_S) + \mathcal{R} I^\alpha + R_0 I$. Since the experimental $\max \mathrm{Re}Z(U_b)$ value is the differential resistance of the entire test structure, is corresponds to the current derivative of U_b:

$$R(U_b) = \frac{dU_b}{dI} = \frac{\phi}{I_S + I} + \frac{\alpha \mathcal{R}}{I^{1-\alpha}} + R_0. \tag{2}$$

Current I in expression (2) should be substituted with (1), where unknown function $U_V(U_b)$ may be expanded as a power series: $U_V(U_b) = bU_b + cU_b^2 + \ldots$. As will be shown below, it is sufficient in the presence case to limit ourselves to linear term $U(U_b) \approx bU_b$

$$R(U_b) = \frac{\phi}{I_S} e^{\frac{(b-1)U_b}{\phi}} + \frac{\alpha \mathcal{R}}{I_S(e^{(1-b)U_b/\phi} - 1)^{1-\alpha}} + R_0. \tag{3}$$

It can be seen from Fig. 2, which shows the plot of function (3), that experimental maxReZ points lie fairly close to the curve representing formula (3). Therefore, the maxReZ value does indeed decrease at higher U_b due to lowering of the Schottky barrier at the Si@O@Al side and weakening of the Si@O@Al varistor effect.

The Nyquist plot for the Ti—$LiCoO_2$—Ti test structure (Fig. 3) consists of two semicircles that are fairly easy to identify. The plot itself may be characterized as the impedance of the structural model shown in the inset of Fig. 3. The corresponding Nyquist plot is represented by gray circles in Fig. 3. The best-fit parameters of the model are $R_1 = 240\,\Omega$, $R_2 = 20\,\Omega$, and $C_1 = C_2 = 2.0 \cdot 10^{-6}$ F. CVCs of the test structure were examined in order to find a reliable interpretation of the obtained data. The CVC analysis revealed that dependence $I(U)$ is non-exponential and is instead characterized by expression

$$I = (U/\mathcal{R}_0)^{1/\alpha} + U/(\mathcal{R}_1 I^{\alpha-1} + R_2).$$

The best approximation is achieved at $\mathcal{R}_0 = 1.5\,\Omega \cdot \mathrm{A}^{1-\alpha}$, $\mathcal{R}_1 = 0.082\,\Omega \cdot \mathrm{A}^{1-\alpha}$, $R_2 = 20\,\Omega$, and $\alpha = 0.26$. The values of resistances $R_0(U_b)$ and $R_1(U_b)$ at $U_b = 5$ mV are 17.2 MΩ and 240 Ω, respectively. Resistance R_0 models the resistance to electron current through a system of percolation clusters. This circuit does not include the contact resistance, since an enriched layer forms at the boundaries. It is evident that resistance R_1 corresponds to hole current, while R_2 is the resistance of a depletion layer.

The concept of resistivity may be used to characterize the resistance of materials with a varistor effect. By definition, the expression for resistivity in this case is $\rho = (\mathcal{R} S^\alpha/h) j^{\alpha-1} + R_0 S/h$ (or, in a more compact form, $\rho = \beta j^{\alpha-1} + \rho_0$), where j is the current density and S and h are the film area and thickness. Measurements of resistivity then boil down to determining the values of parameters β, ρ_0, and α. In the case of Si@O@Al, $\mathcal{R} = 1.56\,\Omega \cdot \mathrm{A}^{1-\alpha}$, $\beta = 8.67 \cdot 10^4\,\Omega \cdot \mathrm{A}^{1-\alpha} \cdot \mathrm{cm}^{2\alpha-1}$, and $\alpha = 0.45$. For $LiCoO_2$ $\mathcal{R}_1 = 0.082\,\Omega \cdot \mathrm{A}^{1-\alpha}$, $\beta = 1.640 \cdot 10^3\,\Omega \cdot \mathrm{A}^{1-\alpha} \cdot \mathrm{cm}^{2\alpha-1}$, $\alpha = 0.26$.

Our findings suggest the following conclusions.

1. Since a backward-biased Ti−Si@O@Al contact has a high differential resistance, the Ti—Si@O@Al—Ti resistance determined by EIS with zero bias is overestimated by three orders of magnitude.

2. A Ti−$LiCoO_2$ contact is ohmic, and CVC nonlinearity is caused by the varistor effect, which is triggered by the nanocrystalline structure of a lithium cobaltite film. The impedance spectrum of Ti—$LiCoO_2$—Ti with zero bias is shaped by the bulk (240 Ω) and contact (20 Ω) resistances.

3. The above two paragraphs suggest that the characteristics of Si@O@Al obtained in [8] should be attributed to $LiCoO_2$ (and vice versa).

4. The results of EIS and CV measurements of the resistance of $LiCoO_2$ agree with each other well, but still exceed the values reported in [10]. This is likely attributable to the nanocrystalline structure of $LiCoO_2$ films.

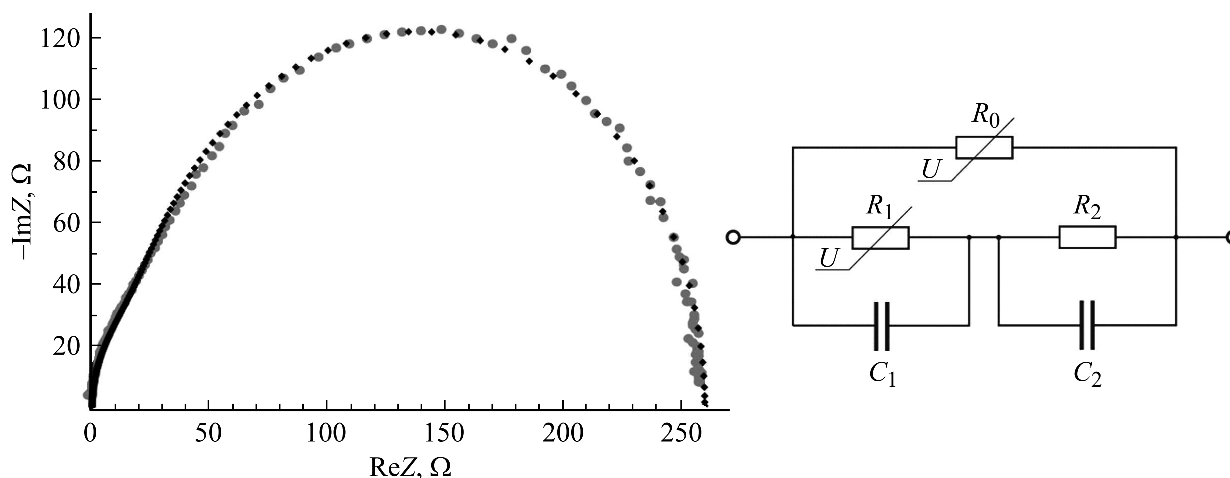

Figure 3. Nyquist plot for the Ti—$LiCoO_2$—Ti test structure and its structural model. The frequency range is 0.5 Hz−500 kHz. Black diamonds are experimental points, and gray circles correspond to the approximating curve. The Nyquist plot was generated at the following parameters of the structural model: $R_0 = 17.2\,\text{M}\Omega$, $R_1 = 240\,\Omega$, $R_2 = 20\,\Omega$, $C_1 = 2.0 \cdot 10^{-6}$ F, and $C_2 = 2.0 \cdot 10^{-6}$ F. The indicated varistor resistances R_0, R_1 correspond to a bias voltage of 5 mV.

Funding

This study was supported financially by the Ministry of Science and Higher Education of the Russian Federation under state assignment No. 0856-2020-0006 for the Demidov Yaroslavl State University.

Conflict of interest

The authors declare that they have no conflict of interest.

References

[1] Y.-N. Zhou, M.-Z. Xue, Z.-W. Fu, J. Power Sources, **234**, 310 (2013). DOI: 10.1016/j.jpowsour.2013.01.183
[2] X. Zuo, J. Zhu, P. Müller-Buschbaum, Y.-J. Cheng, Nano Energy, **31**, 113 (2017). DOI: 10.1016/j.nanoen.2016.11.013
[3] K. Feng, M. Li, W. Liu, A.G. Kashkooli, X. Xiao, M. Cai, Z. Chen, Small, **14** (8), 1702737 (2018). DOI: 10.1002/smll.201702737
[4] W.-J. Zhang, J. Power Sources, **196** (1), 13 (2011). DOI: 10.1016/j.jpowsour.2010.07.020
[5] J.R. Szczech, S. Jin, Energy Environ. Sci., **4** (1), 56 (2011). DOI: 10.1039/C0EE00281J
[6] B. Liang, Y. Liu, Y. Xu, J. Power Sources, **267**, 469 (2014). DOI: 10.1016/j.jpowsour.2014.05.096
[7] A.A. Mironenko, I.S. Fedorov, A.S. Rudy, V.N. Andreev, D.Yu. Gryzlov, T.L. Kulova, A.M. Skundin, Monatsh. Chem., **150** (10), 1753 (2019). DOI: 10.1007/s00706-019-02497-1
[8] A.S. Rudyi, S.V. Kurbatov, A.A. Mironenko, V.V. Naumov, Yu.S. Egorova, Pis'ma Zh. Tekh. Fiz., **49** (7), 20 (2023) (in Russian). DOI: 10.21883/PJTF.2023.07.54916.19431
[9] A.S. Rudy, A.B. Churilov, A.A. Mironrenko, V.V. Naumov, S.V. Kurbatov, E.A. Kozlov, Tech. Phys. Lett., **48** (9), 7 (2022). DOI: 10.21883/TPL.2022.09.55072.19276.
[10] D.G. Kellerman, V.R. Galakhov, A.S. Semenova, Ya.N. Blinovskov, O.N. Leonidova, Phys. Solid State, **48** (3), 548 (2006). DOI: 10.1134/S106378340603022X.
[11] Y. Iriyama, T. Kako, C. Yada, T. Abe, Z. Ogumi, J. Power Sources, **146** (1-2), 745 (2005). DOI: 10.1016/j.jpowsour.2005.03.073
[12] Y. Iriyama, T. Kako, C. Yada, T. Abe, Z. Ogumi, Solid State Ion., **176** (31-34), 2371 (2005). DOI: 10.1016/j.ssi.2005.02.025
[13] S.D. Fabre, D. Guy-Bouyssou, P. Bouillon, F. Le Cras, C. Delacourta, J. Electrochem. Soc., **159** (2), A104 (2012). DOI: 10.1149/2.041202jes
[14] S. Larfaillou, D. Guy-Bouyssou, F. Le Cras, S. Franger, ECS Trans., **61** (27), 165 (2014). DOI: 10.1149/06127.0165ecst

Translated by D.Safin